Video Article

Fabrication of a Multiplexed Artificial Cellular MicroEnvironment Array

Yasumasa Mashimo[1,2], Momoko Yoshioka[1], Yumie Tokunaga[1], Christopher Fockenberg[1], Shiho Terada[1], Yoshie Koyama[1], Teiko Shibata-Seki[2], Koki Yoshimoto[1], Risako Sakai[1], Hayase Hakariya[1], Li Liu[1], Toshihiro Akaike[3], Eiry Kobatake[2], Siew-Eng How[4], Motonari Uesugi[1,5], Yong Chen[1,6], Ken-ichiro Kamei[1]

[1]Institute for Integrated Cell-Material Sciences (WPI-iCeMS), Kyoto University

[2]Department of Life Science and Technology, School of Life Science and Technology, Tokyo Institute of Technology

[3]Biomaterials Center for Regenerative Medical Engineering, Foundation for Advancement of International Science

[4]Faculty of Science and Natural Resources, Universiti Malaysia Sabah

[5]Institute for Chemical Research, Kyoto University

[6]Ecole Normale Supérieure

Correspondence to: Ken-ichiro Kamei at kkamei@icems.kyoto-u.ac.jp

URL: https://www.jove.com/video/57377
DOI: doi:10.3791/57377

Keywords: Bioengineering, Issue 139, microfluidic, nanofiber, embryonic stem cell, cellular microenvironment, single-cell profiling, self-renewal

Date Published: 9/7/2018

Citation: Mashimo, Y., Yoshioka, M., Tokunaga, Y., Fockenberg, C., Terada, S., Koyama, Y., Shibata-Seki, T., Yoshimoto, K., Sakai, R., Hakariya, H., Liu, L., Akaike, T., Kobatake, E., How, S.E., Uesugi, M., Chen, Y., Kamei, K.i. Fabrication of a Multiplexed Artificial Cellular MicroEnvironment Array. *J. Vis. Exp.* (139), e57377, doi:10.3791/57377 (2018).

Abstract

Cellular microenvironments consist of a variety of cues, such as growth factors, extracellular matrices, and intercellular interactions. These cues are well orchestrated and are crucial in regulating cell functions in a living system. Although a number of researchers have attempted to investigate the correlation between environmental factors and desired cellular functions, much remains unknown. This is largely due to the lack of a proper methodology to mimic such environmental cues *in vitro*, and simultaneously test different environmental cues on cells. Here, we report an integrated platform of microfluidic channels and a nanofiber array, followed by high-content single-cell analysis, to examine stem cell phenotypes altered by distinct environmental factors. To demonstrate the application of this platform, this study focuses on the phenotypes of self-renewing human pluripotent stem cells (hPSCs). Here, we present the preparation procedures for a nanofiber array and the microfluidic structure in the fabrication of a Multiplexed Artificial Cellular MicroEnvironment (MACME) array. Moreover, overall steps of the single-cell profiling, cell staining with multiple fluorescent markers, multiple fluorescence imaging, and statistical analyses, are described.

Video Link

The video component of this article can be found at https://www.jove.com/video/57377/

Introduction

Human pluripotent stem cells (hPSCs)[1,2] self-renew unlimitedly and differentiate into various tissue lineages, which could revolutionize drug development, cell-based therapies, tissue engineering, and regenerative medicine[3,4,5,6]. General culture dishes and microtiter plates, however, are not designed to enable precise physical and chemical cell manipulation at the cellular level with the range of nano- to micro-meters, which is a critical factor for cellular expansion, self-renewal, and differentiation. To address this drawback, studies have investigated the roles of cellular microenvironments in regulating cell-fate decisions and cell functions[4]. In recent years, an increasing number of studies have been conducted to reconstruct cellular microenvironments *in vitro*[7,8]. Nano- and micro-fabrication processes have established these microenvironments through the manipulation of chemical[9,10,11,12,13,14,15,16,17] and physical[18,19,20] environmental cues. Until now, there were no reports to systematically investigate the underlying mechanisms of chemical and physical environmental cues on cell-fate decisions and functions within a single platform.

Here, we introduce a strategy based on simple design principles to establish a robust screening platform (**Figure 1**). First, we describe the development procedure of an integrated platform for creating versatile, artificial cellular microenvironments by using a nanofiber array and a microfluidic structure: The Multiplexed Artificial Cellular MicroEnvironment (MACME) array (**Figure 1A** and **2A**). The nanofiber array has 12 different microenvironments in varying combinations of nanofiber materials and densities. Electrospinning was used to fabricate nanofibers. The nanofiber materials, such as polystyrene (PS)[21], polymethylglutarimide (PMGI)[22], and gelatin (GT)[23], were designed to test their chemical properties, which might affect cell adhesion and maintenance of pluripotency (**Figure 2B**). Nanofiber densities were varied by changing electrospinning time and the generated nanofibers were defined according to their densities (DNF, with D = XLow/Low/Mid/High). The microfluidic structure is composed of polydimethylsiloxane (PDMS) harboring 48 cell-culture chambers, which can be positioned along the standard dimensions of the 96-well microplate. PDMS is a biocompatible and gas-exchangeable polymer generally used to fabricate microfluidic devices[24]. Each microfluidic channel was designed to be 700-µm wide and 8.4-mm long and had two inlets at its edges (**Table 1**). The chambers had different heights (250, 500, and 1000 µm) to manipulate the initial cell-seeding densities (0.3, 0.6, and 1.2 × 10^5 cells/cm^2), which might correlate with survival, proliferation, and differentiation of hPSCs[25] (**Figure 2C**). The number of cells seeded into a chamber is proportional to the column density above the chamber floor, and thus initial cell seeding density was controlled by introducing the same cell suspension into

culture chambers with different heights. All channels were designed to be ≥ 250-μm-high[26] to minimize the effects of low-oxygen tension[27] and shear stress[28] on the cells. Channel heights of 250, 500, and 1000 μm are abbreviated here as XCD with X = Low, Mid, and High, respectively. The environments with distinct nanofiber densities and initial cell-seeding densities were shortened as "Material_NF density_Cell density" (e.g., GT_HighNF_HighCD: an environment characterized by high-density GT nanofibers and high initial cell-seeding density).

Subsequently, we describe how to perform single-cell analyses to systematically investigate cell behavior in response to environmental factors (**Figure 1B**). As a proof-of-concept, we identified the optimal cellular environment for hPSC self-renewal, which is a key function for hPSC maintenance (**Figure 1B**)[29]. Image-based cytometry, followed by statistical analyses, allows for quantitative interpretation of individual cellular phenotypic responses to cellular environments. Among a variety of cellular functions, this paper provides a detailed procedure to identify the optimal conditions for maintaining hPSC self-renewal.

Protocol

1. Fabrication of MACME Array

Note: All materials and equipment are listed in the Materials Table.

1. **Preparation of masks for a nanofiber array and a mold for a microfluidic structure**
    1. Create three-dimensional (3D) images of masks used for the nanofiber arrays and molds for microfluidic structures using 3D-computer graphics software packages (**Table 1**).
    Note: The 3D images are read and printed by a 3D printer. The printed masks and mold have the same dimensions with 3D images defined using the graphics software at step 1.1.1.
    2. Print masks and a mold based on these designs using a 3D printer.
    Note: In this protocol, an ink-jet-like 3D printer with UV-curable resin was used[30]. The printer resolution was 635 × 400 dpi and 15 μm in X, Y and Z, respectively, however, the actual X, Y resolution was approximately four times lower.

2. **Nanofiber-array preparation (Figure 3A)**
    1. Prepare polymer solutions for electrospinning.
        1. Dilute 13% PMGI liquid with tetrahydrofuran by 9% (w/v)[22].
        2. Dissolve 0.08 g of PS (Number-average molecular weight (Mn): 130,000) in THF:dimethylformamide (1:1 volume ratio)[21], and add THF:dimethylformamide to bring the volume up to the final 1 mL (8% (w/v) PS solution).
        3. Dissolve 0.1 g of GT in water:acetic acid:ethyl acetate (1:1.6:2.1 volume ratio), and add water:acetic acid:ethyl acetate to bring the volume up to the final 1 mL (10% (w/v) GT solution) as described[23,31].
    2. Use a magnetron sputtering machine, deposit a thin platinum layer with a 5-nm thickness on a polystyrene (PS) baseplate (127.7 × 85.5 mm), which serves as a cathode in the electrospinning setup.
    3. Load each polymer solution into a 5-mL syringe equipped with a 23-G stainless-steel blunt needle.
    4. Place and anchor the syringe with the needle on a syringe pump with 12-cm apart from the collector of the electrospinning device.
    5. Connect the syringe needle to a high-voltage power supply, and set to apply to 11 kV.
    6. Set the pumping rate of 0.2 mL/h.
    7. Keep temperature and humidity at 30 °C and < 30% (v/v).
    8. Put the mask on the baseplate prepared at step 1.2.2.
    9. Fabricate nanofibers on the baseplate through the holes of mask with distinct densities by changing the electrospinning time (e.g., 20, 60, 90, and 180 s).
    10. Remove the mask from the baseplate.
    Note. Ethanol can be sprayed on the electrospun GT nanofibers before removing the mask to avoid peeling off GT nanofibers together with the mask.
    11. Repeat step 1.2.4-1.2.10 until the completion of nanofiber-array fabrication.
    12. Place the nanofiber array in a desiccator at 25 °C for 16 h to evaporate the remaining solvent.
    13. Crosslink GT nanofibers with 0.2 M 1-ethyl-3-(3-dimethylaminopropyl) carbodiimide hydrochloride (EDC) and 0.2 M N-hydroxysuccinimide (NHS) in ethanol at 25 °C for 4 h[23].
    14. Rinse GT nanofibers twice with 99.5% (v/v) ethanol and vacuum-dry at 25 °C for 16 h.

3. **Fabrication of microfluidic structures (Figure 3B)**
    1. Mix 2 g of PDMS curing agent and 20 g of PDMS base (1:10 weight ratio; Pre-PDMS). [24]
    2. Pour the pre-PDMS mixture onto the mold fabricated in step 1.2.
    3. De-gas the pre-PDMS mixture in a desiccator for 30 min.
    4. Cure the pre-PDMS mixture in an oven at 65 °C for 16 h.

4. **Assembly of MACME arrays (Figure 3B)**
    1. Peel off the PDMS structure cured at step 1.3.4 from the mold and clean with 70% (v/v) ethanol.
    2. Treat atmospheric corona discharge on the bottom side of the PDMS structure[32].
    Note: In this protocol, the corona is discharged on the entire surface of a layer 3 or 4 times with a "Handy" corona discharge apparatus. Oxygen plasma treatment was replaced with atmospheric corona discharge to alter the surface adhesiveness.
    3. Assemble the PDMS structure with the nanofiber array quickly.
    4. Oven-bake at 65°C for 2 days.

2. Loading hESCs into MACME Array

1. For the routine culture of H9 human embryonic stem cells (hESCs), maintain cells in xeno-free chemically defined culture medium for hPSC maintenance[33] supplemented with 10 μM Y-27632 ROCK inhibitor[34] (named hPSC medium) in a 35-mm cell culture dish coated with basement membrane gel matrix (MG).
2. Passage cells every 4 to 7 days using a recombinant trypsin-like protease.
3. Sterilize a MACME array with 99.5% ethanol, by loading into the chambers for 10 min, and then remove the ethanol. Repeat this step 3 times.
4. Introduce 12 μL of MG, 10 μg/mL vitronectin (VN), and 0.1% (w/v) GT into control culture chambers, and incubate the chambers at 37 °C for 1 h to coat them on the chamber surfaces.
   Note: In this protocol, MG, VN, and GT were selected as reference proteins for cell adhesion and culture. Because MG and VN are standard cell-culture matrices used for maintaining hPSC self-renewal, they are used as positive controls; two-dimensional GT coating (2DGT) or non-coating (NC) were used as negative controls.
5. Introduce pre-warmed hPSC medium into all chambers of MACME array. Incubate the chambers for 30 min at 37 °C.
6. Wash H9 hESC cultured on a 35-mm dish with DPBS, add 0.5 mL of a recombinant trypsin-like protease to the dish and incubate at 37 °C for 1 min and carefully aspirate only the supernatants mixed with protease.
   Note: At the aspiration step, the cells are not detached.
7. Immediately add hPSC medium, gently dispense the medium against the dish surface repeatedly to dissociate cells and transfer the detached cells to a 15-mL conical tube.
8. Centrifuge at 200 x g for 3 min. Aspirate the supernatant and suspend cells in a pre-warmed hPSC medium.
9. Introduce 12 μL of the cell suspension (1.2×10^6 cells/mL) into each microfluidic chamber.
   Note: Introduce cells to one chamber from another using a micropipette. Because the number of cells seeded to chambers is proportional to the column density above the chamber floor, the initial cell-seeding density could be controlled even though samples from same cell suspension were used. Ensure pipetting is done gently. Remove excess medium from the chambers using a cotton-tipped stick after loading. The MACME array is compatible with both commonly used laboratory pipettes and automated pipette systems, and it does not require any special equipment.
10. Change hPSC medium every 12 h and culture for 4 days.
    Note: Constant volumes of the medium (1.6, 3.2, and 6.4 μL) are maintained by using chambers of distinct sizes. Culture cells under a static condition to minimize shear stress except for the exchanging of the cell culture medium[35,36].

3. Quantitative Single-cell Profiling

1. **On-plate fluorescent cell staining**
   Note: To analyze phenotypic changes of self-renewing hPSCs, this protocol selected three key phenotypic markers for this protocol: OCT4, 5-ethynyl-2'-deoxyuridine (EdU), and Annexin V, to measure the status of pluripotency, proliferation, and apoptosis, respectively (**Figure 2b**). 4',6-diamidino-2-phenylindole (DAPI) is used to identify cell nuclei. OCT4 is one of the critical transcription factors of pluripotency.
   1. Incubate H9 hESCs in MACME arrays in hPSC medium supplemented with 10 μM EdU alkyne at 37 °C for 30 min.
   2. After washing with annexin-binding buffer (10 mM HEPES (pH 7.4), 140 mM NaCl, 2.5 mM $CaCl_2$), stain the cells with an orange-fluorescent dye-Annexin V conjugate at 20 °C for 15 min.
   3. Fix cells in PBS with 4% (v/v) paraformaldehyde at 20 °C for 15 min, and then rinse cells with PBS twice.
   4. Permeabilize cells using PBS with 0.3% (v/v) Triton X-100 at 20 °C for 16 h.
      Note: Paraformaldehyde weakens the bond between a plastic base plate and a PDMS microfluidic structure. Thus, the detachment of the PDMS layer from the array at step 3.2.1 can also be performed right after this step.
   5. Incubate cells in Tris-based reaction buffer with a red-fluorescent dye azide at 20 °C for 30 min.
   6. Incubate cells in blocking buffer (PBS with 5% (v/v) normal goat serum, 5% (v/v) normal donkey serum, 3% (w/v) bovine serum albumin, 0.1% (v/v) Tween-20, and 0.1% (w/v) N-dodecyl-β-D-maltoside) at 4 °C for 16 h.
   7. Incubate in PBS with 0.5% (v/v) Triton X-100 solution and human OCT3/4 antibody (mouse IgG) at 4 °C for 16 h.
   8. Incubate in blocking buffer with green-fluorescent dye-labeled donkey anti-mouse IgG (H+L) at 37°C for 60 min.
   9. Incubate in PBS with DAPI at 20 °C for 30 min.
   10. Replace PBS-DAPI with PBS.
   11. Preserve the MACME array at 4 °C until image acquisition.

2. **Image acquisition (Figure 4)**
   1. Peel off the PDMS microfluidic structure from the MACME array.
   2. Remove the residual PBS from the MACME array, apply 90%(v/v) glycerol in PBS to the cells and place coverslips over the stained cells.
   3. Set the plate upside down on the stage of an inverted fluorescence microscope.
   4. Acquire 12-bit color images automatically using all motorized components (stage, filters, shutter, and focus systems) that were controlled by a microscope imaging software.
      Note. In this protocol, exposure times are adjusted to reach near maximum intensity values (highest pixel intensity: 4096), but no saturation, for each image, DAPI, OCT4, Annexin V, and EdU.

3. **Computer-guided image processing and fluorescence signal quantification (Figure 5)**
   Note: The following cell image analysis is performed based on a previously described method[37].
   1. Convert color images to grayscale.
   2. Calculate a single threshold value for each DAPI image with the Otsu method and classify pixels above the threshold as foreground and below as background. Ensure that the foreground value corresponds to the fluorescent intensity of DAPI.
      Note: The image analysis process contains 5 steps; identification of primary objects in DAPI images, identification of secondary objects in OCT4, Annexin V, and EdU images, respectively, and measurement of object intensity. **Figure 3** provides the images of graphical user interface (GUI) on the setting of image processing.

3. Measure the fluorescent intensities of OCT4 and EdU on each image.
4. Identify the region stained with Annexin V with the propagation method, and quantify the fluorescent intensity.

4. **3.4. Statistical analysis to visualize individual cellular phenotypes on single-cell imaging**
   1. Normalize the input fluorescent intensities of each phenotypic marker by centering and scaling these variables to give them equal weight.
   2. Perform self-organizing map (SOM) analysis by using a software environment for statistical computing and graphics as described by previous studies[38,39].
      1. Create 25 SOM nodes with distinctive four "codebook vectors" corresponding to the fluorescent intensities of four markers, DAPI, EdU, Annexin V, and OCT4.
      2. Assign individual cells in each microenvironment to a "winning" (most similar) node, and plot as cell frequency, according to which the codebook vectors of the winning node are updated using a weighted average, where the weight is the learning rate (here, 0.05 as default).
         Note: Omit data from chambers containing less than 1,000 cells because datasets containing a few cells did not provide statistically relevant SOM results.
   3. Perform unsupervised hierarchical clustering with the SOM-node values using the average-linkage method based on Pearson correlation by a clustering software[40].
   4. Render the clustering data into dendrogram and heatmap views[41].

Representative Results

MACME arrays: Design and fabrication: In combination with nanofiber technology, we used microfluidic cell culture and screening techniques employed previously to identify optimal conditions for hPSC self-renewal or differentiation[35,36] (**Figure 1**). This is well suited for establishing robust high-throughput cell-based assays because the cell culture chambers and conditions are precisely controllable and expandable[42,43,44]. Here, the nanofiber array was prepared by a simple nanofiber deposition method, electrospinning with 3D-printed masks. The microfluidic part was fabricated with a 3D-printed mold to easily design the chamber structure through many trials and errors. The MACME array was constructed by combining the two parts and contained 48 environments, providing different biophysical and biochemical cues by varying combinations of both nanofiber ECMs (3 types of nanofiber materials and 4 different densities or 4 control matrix proteins) and cell-cell interactions (3 ranges of initial cell-seeding density) as shown in **Figure 2**.

Evaluation of overall effects of nanofiber properties and cellular density on hESC phenotypes: Following cell culture on a MACME array and on-plate fluorescent staining (**Figure 6A**), single-cell measurements were performed with the acquired images. For comparing homogeneity and heterogeneity of expression levels for the four phenotypic markers in each dataset, this protocol used SOM analysis[38,39], which converts high-dimensional, multiparametric datasets into low-dimensional 2D maps. Notably, the results of PS nanofibers and 2DGT matrices were omitted from this analysis given that most cells did not adhere. Moreover, excluded from this analysis were those experiments with low CD where cells did not have enough direct (e.g., juxtacrine) or indirect (paracrine) interactions to survive. Following SOM analysis, unsupervised hierarchical clustering was performed for the SOM nodes of all analyzed samples (**Figure 6B**). By considering the height of the cluster dendrogram, the phenotypic differences allowed us to categorize the samples into three groups: Group i, most of the sample niches comprising of GT nanofibers, MG_HighCD, and VN_HighCD; Group ii, samples containing GT nanofibers (GT_XLow and MidNF_MidCD), MG_MidCD, or VN_MidCD; and Group iii, all PMGI_NF samples.

To study the differences among the groups, we examined one representative sample from each group (**Figure 6C**; Group i-GT_MidNF_HighCD, Group ii-GT_MidNF_MidCD, and Group iii-PMGI_MidNF_HighCD). In terms of OCT4 signals, all groups showed a higher expression than that of MG (MG_MidCD). Group i was characterized by high EdU signals, indicating that most cells were actively proliferating. Thus, microenvironments in Group I were characterized as conditions suitable for hPSC maintenance because undifferentiated hPSCs typically proliferate rapidly when cell-cycle gap phases were shortened[45,46].

GT_MidNF_HighCD and GT_MidNF_MidCD are distinguished by their distinct initial cell-loading densities. High initial cell densities increased cells' opportunities to interact with neighboring cells, which enhanced their survival and proliferation[47]. Cells seeded at an insufficient initial density (3.0×10^4 cells/cm^2) neither survived nor grew during the experimental period (4 days). Therefore, we did not incorporate these samples in the SOM analysis; cell numbers were below the cut-off of 1000 living cells/chamber. The cells on 2DGT scaffolds were also categorized as Group ii cells; these conditions do not support hPSC self-renewal[48]. The GT_MidNF_MidCD cells' EdU signal was lost and Annexin V levels were slightly increased, indicating that the cells had lost their stemness and had gradually become apoptotic. PMGI_MidNF_HighCD, which represents the microenvironments comprising PMGI nanofiber matrices, showed the larger variations in OCT4 and EdU signals compared with the other conditions.

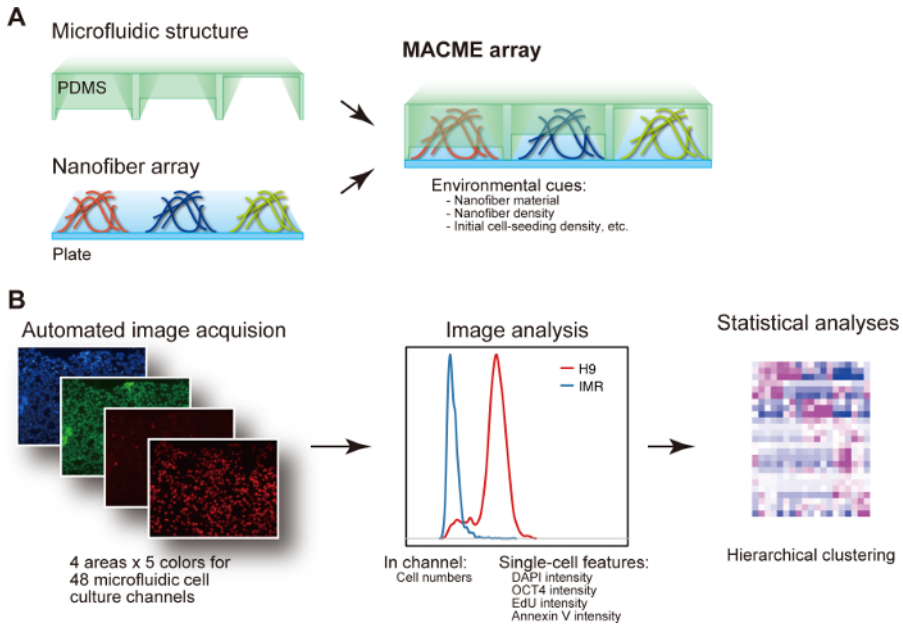

Figure 1. Screening strategy to identify optimal cellular microenvironments for regulating cellular functions. (**A**) Overview of the components of the multiplexed artificial cellular microenvironment (MACME) array. The array is comprised of two main parts: nanofiber beds patterned on a basal substrate (nanofiber array) and a polydimethylsiloxane (PDMS)-based microfluidic structure. The MACME array is able to prepare nanofiber ECMs with a variety of features (i.e., nanofiber materials and densities) and various cell seeding densities. The PDMS microfluidic structure of the MACME array features three microfluidic-channel heights (250, 500, and 1000 µm) to regulate the initial cell-seeding density. (**B**) The impact of cellular microenvironments on cell phenotypes is quantitatively evaluated using an image-based single-cell assay and the statistical data analysis by self-organizing map (SOM) followed by hierarchical clustering. This figure was adapted from reference[49] with permission from Wiley. Please click here to view a larger version of this figure.

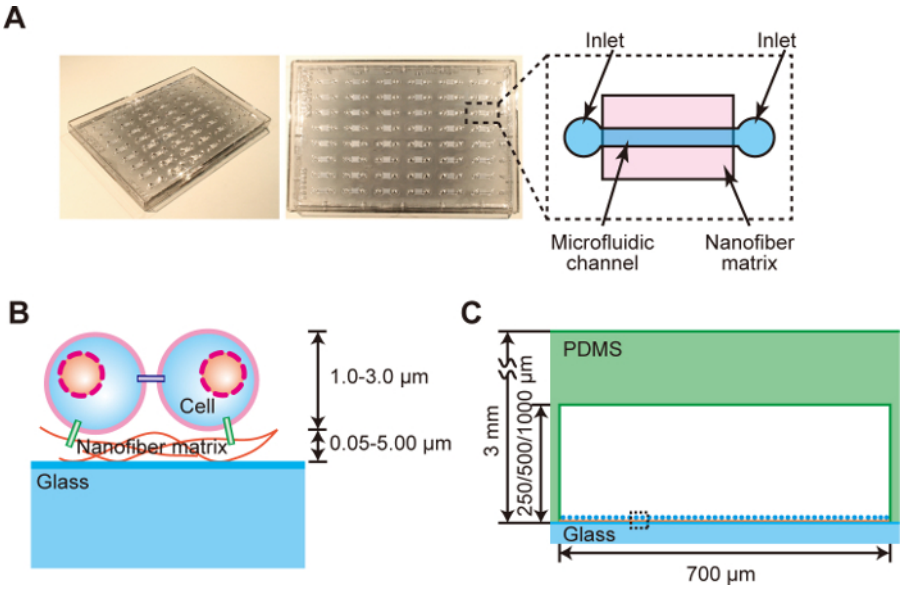

Figure 2. Design of the MACME array. (**A**) Overhead and high-angle shots of the entire MACME array and the conceptual diagram of a microfluidic channel (light blue) on a nanofiber matrix (pink). Each channel is composed of a 700 µm wide and 8.4 mm long culture chamber and two inlets for introduction of medium and cells. (**B**) Comparison of sizes of cells and nanofiber matrices. The heights of cells and nanofiber beds range from 1-3 µm and 0.05-5.0 µm, respectively. (**C**) A cross section of each microfluidic channel with a 250/500/1000 µm height. Cells and nanofiber beds are represented as blue circles and orange lines, respectively. Each chamber has the same width and length but different heights (250, 500, and 1000 µm), and each chamber volume was 1.6, 3.2, and 6.4 µL, respectively. The black dotted rectangle in **Figure 2C** denotes **Figure 2B**. **Figure 2** was adapted from reference[49] with permission from Wiley. Please click here to view a larger version of this figure.

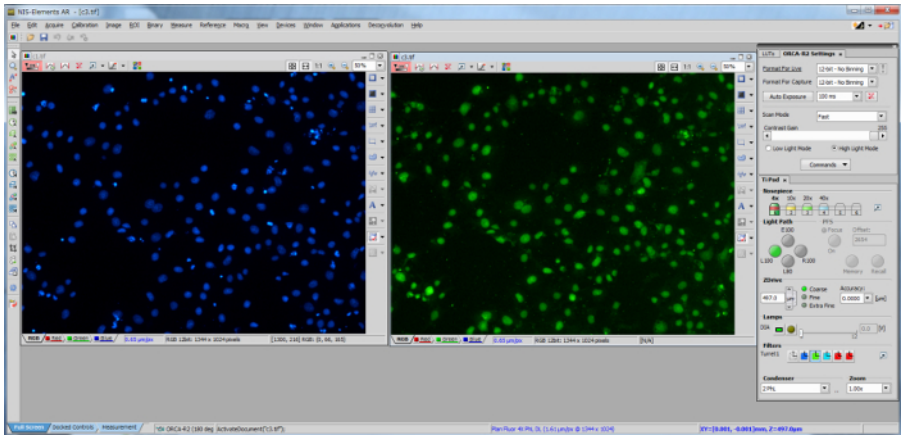

Figure 3. Fabrication of MACME array. (**A**) Fabrication of a nanofiber array. Patterning multiple nanofiber matrices on a baseplate was performed by modified electrospinning using a set of masks bearing patterned holes. Platinum-coating was performed to facilitate nanofiber deposition on a plastic baseplate. The masks with distinct hole-patterns were prepared by a 3D printer. Following masking of the platinum-coated area of the plate, the plate-mask set was put on the collection screen, and normal electrospinning was performed. The initial nanofibers were formed at the Pt-coated positions on the plate through the holes in the mask. Additional nanofiber beds were fabricated on the plate by replacing the existing mask and repeating the procedure. (**B**) Fabrication of a microfluidic structure. The mold printed by a 3D printer with UV-curable resin shaped the PDMS layer of the microfluidic device. After casting, the MACME array was assembled by attaching a PDMS-based microfluidic layer with a surface-activated nanofiber array. **Figure 3** was adapted from reference[49] with permission from Wiley. Please click here to view a larger version of this figure.

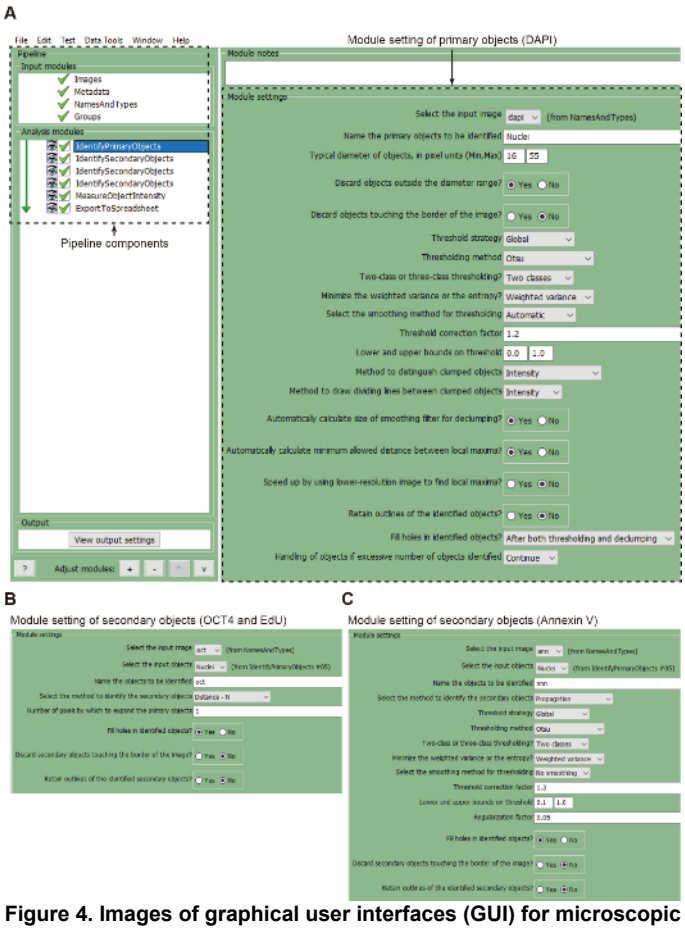

Figure 4. Images of graphical user interfaces (GUI) for microscopic image acquisition. Please click here to view a larger version of this figure.

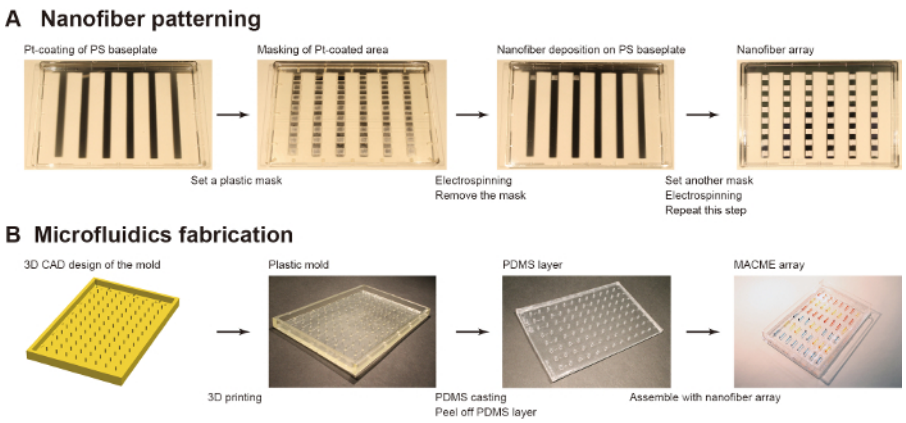

Figure 5. Images of graphical user interfaces (GUI) of computer-guided image processing for single-cell phenotyping. The image analysis process contains 5 steps; (**A**) identification of primary objects in DAPI images, (**B-D**) identification of secondary objects in OCT4, Annexin V and EdU images, respectively, and measurement of object intensity. Please click here to view a larger version of this figure.

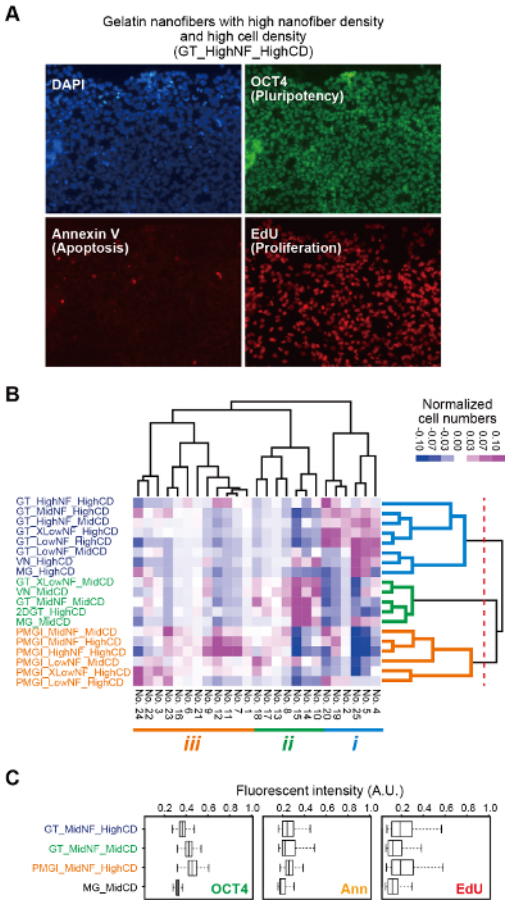

Figure 6. Phenotyping and classification of the phenotypes of H9 hESCs altered by microenvironmental factors. (**A**) Immunofluorescent images of H9 hESCs cultured at high initial seeding density on gelatin (GT) nanofibers (GT_HighNF_HighCD), stained with three cellular phenotypic markers (OCT4, pluripotency; EdU, cell proliferation; Annexin V, apoptosis) and DAPI for cell nuclei. (**B**) A heatmap and dendrograms of unsupervised hierarchical clustering. The tested microenvironments were categorized into three groups with distinctive features based on similarities of the phenotypes. Group i included GT nanofibers, MG_HighCD, and VN_HighCD. Group ii consisted of samples of GT nanofibers (GT_XLow and MidNF_MidCD), MG_MidCD, or VN_MidCD. All PMGI_NF samples were clustered into Group iii. In the heatmap, pink and blue colors indicate high and low cellular frequencies in SOM count plots, respectively. (**C**) Distribution of quantified marker expression levels of 1000 cells in one representative sample from each group (Group i-GT_MidNF_HighCD, Group ii-GT_MidNF_MidCD, and Group iii-PMGI_MidNF_HighCD). The 25th and 75th percentiles were indicated as the box limits. The whiskers extend to 1.5 times the interquartile range from the 25th and 75th percentiles. Experiments were repeated three times for each group. **Figure 6A-C** were adapted from reference[49] with permission from Wiley. Please click here to view a larger version of this figure.

Name	Channel length (mm)	Channel width (μm)	Channel height (μm)	Inlet/Outlet diameter (μm)	Inlet/Outlet height (μm)	Mould length (mm)	Mould width (mm)	Mould height (mm)
Mold	8.4	700	250/500/1000	800	3000	127.76	85.48	14.35
Name	**Thickness (μm)**	**Hole length (mm)**	**Hole width (mm)**	**Mask length (mm)**	**Mask width (mm)**	**Mould height (mm)**	**Row Offset (mm)**	**Column Offset (mm)**
Mask	1000	6	5	123.5	80.2	14.35	11.24	14.38

Table 1. Dimensions of mold for a microfluidic structure and mask for a nanofiber patterning.

Discussion

This protocol demonstrates the first screening method to establish a robust culture system for the maintenance of qualified hPSCs. First, we described how to prepare a platform featuring diverse artificial ECMs and cell seeding densities by using a microfluidic device integrated with a nanofiber array, the MACME array. Second, quantitative image-based single-cell phenotyping was performed[50] to evaluate individual cellular outcomes and behaviors altered by distinct biochemical and biophysical features. In this protocol, the environment consisting of GT nanofiber and positive control ECM proteins in the condition of high initial cell seeding density was characterized by features of an undifferentiated state; rapid proliferation[45] and stable OCT4 expression[51]. This observation indicated that molecular mechanisms relating to "cell-extracellular matrix" and "cell-cell" interactions could affect pluripotency of hPSCs.

This strategy can be customized to suit the user's purpose. For example, cell manipulation and throughput can be adjusted for a variety of experimental settings by re-designing the shapes and patterns of the microfluidic structure. As another way for throughput improvement, the inlet and outlet positions of each chamber are designed as per the microplate standard of 96-well plates, standardized by the Society of Biomolecular Sciences; thus, an automated robotic liquid dispenser can be used for high-throughput screening. To further examine the molecular mechanism concerning "cell-ECM interactions", the artificial cellular microenvironments can be made to more precisely mimic *in vivo* conditions by chemically modifying the nanofibers with signaling molecules[52].

To date, most platforms developed for screening cellular microenvironments have been aimed at screening soluble factors (e.g., growth factors and chemical compounds)[42,43,44], but not nanofiber ECMs owing to difficulties in combining the distinct fabrication techniques. For example, a nanofiber sheet produces a small gap between a microfluidic structure and a baseplate and causes their unstable bonding, which results in cross-contamination between different samples because a culture medium mix with another chamber's one through the small gap. Our new method facilitates simple and precise fabrication of nanofiber matrices at specific sites and allows their direct bonding with the baseplate, which prevents both unstable bonding and cross-contamination. Moreover, few platforms[53] integrated with microfluidics and nanofiber matrices have been accessible for the systematic manipulation of both chemical and physical cues to investigate their effects on cell functions, because technologies needed for the integration were highly sophisticated. Our single-cell profiling with the MACME array can be performed with an easily attainable apparatus and simple techniques and holds great potential for use in modeling cellular environments for developmental and cell biological studies and drug discovery/screening.

Disclosures

None.

Acknowledgements

We thank Prof. N. Nakatsuji at iCeMS, Kyoto University, for providing human ES cells. We also thank Prof. A. Maruyama at Tokyo Institute of Technology for his support in the use of the atomic force microscope. Funding was generously provided by the Japan Society for the Promotion of Science (JSPS; 22350104, 23681028, 25886006, and 24656502); funding was also provided by the New Energy and Industrial Technology Development Organization (NEDO) and the Terumo Life Science Foundation. The WPI-iCeMS is supported by the World Premier International Research Centre Initiative (WPI), the Ministry of Education, Culture, Sports, Science and Technology (MEXT), Japan. A part of this work was supported by Kyoto University Nanotechnology Hub and the AIST Nano-Processing Facility in "Nanotechnology Platform Project" sponsored by MEXT, Japan.

References

1. Thomson, J. A. *et al.* Embryonic stem cell lines derived from human blastocysts. *Science.* **282** (5391), 1145-1147 (1998).
2. Takahashi, K. *et al.* Induction of pluripotent stem cells from adult human fibroblasts by defined factors. *Cell.* **131** (5), 861-872 (2007).
3. Ameen, C. *et al.* Human embryonic stem cells: Current technologies and emerging industrial applications. *Crit Rev Oncol Hematol.* **65** (1), 54-80 (2008).
4. Nishikawa, S., Goldstein, R. A., & Nierras, C. R. The promise of human induced pluripotent stem cells for research and therapy. *Nat Rev Mol Cell Biol.* **9** (9), 725-729 (2008).
5. Robinton, D. A., & Daley, G. Q. The promise of induced pluripotent stem cells in research and therapy. *Nature.* **481** (7381), 295-305 (2012).
6. Sartipy, P., Bjorquist, P., Strehl, R., & Hyllner, J. The application of human embryonic stem cell technologies to drug discovery. *Drug Discovery Today.* **12** (17-18), 688-699 (2007).
7. Discher, D. E., Mooney, D. J., & Zandstra, P. W. Growth factors, matrices, and forces combine and control stem cells. *Science.* **324** (5935), 1673-1677 (2009).

8. Joyce, J. A., & Pollard, J. W. Microenvironmental regulation of metastasis. *Nat Rev Cancer.* **9** (4), 239-252 (2009).
9. Danhier, F., Feron, O., & Preat, V. To exploit the tumor microenvironment: Passive and active tumor targeting of nanocarriers for anti-cancer drug delivery. *J Control Release.* **148** (2), 135-146 (2010).
10. Murphy, W. L., McDevitt, T. C., & Engler, A. J. Materials as stem cell regulators. *Nat Mater.* **13** (6), 547-557 (2014).
11. Patel, A. K. *et al.* A defined synthetic substrate for serum-free culture of human stem cell derived cardiomyocytes with improved functional maturity identified using combinatorial materials microarrays. *Biomaterials.* **61** 257-265 (2015).
12. Zhang, R. *et al.* A thermoresponsive and chemically defined hydrogel for long-term culture of human embryonic stem cells. *Nat Commun.* **4** (2013).
13. Anderson, D. G., Putnam, D., Lavik, E. B., Mahmood, T. A., & Langer, R. Biomaterial microarrays: rapid, microscale screening of polymer-cell interaction. *Biomaterials.* **26** (23), 4892-4897 (2005).
14. Celiz, A. D. *et al.* Discovery of a Novel Polymer for Human Pluripotent Stem Cell Expansion and Multilineage Differentiation. *Adv Mater.* **27** (27), 4006-4012 (2015).
15. Hansen, A. *et al.* High-Density Polymer Microarrays: Identifying Synthetic Polymers that Control Human Embryonic Stem Cell Growth. *Adv Healthcare Mater.* **3** (6), 848-853 (2014).
16. Mei, Y. *et al.* A high throughput micro-array system of polymer surfaces for the manipulation of primary pancreatic islet cells. *Biomaterials.* **31** (34), 8989-8995 (2010).
17. Saha, K. *et al.* Surface-engineered substrates for improved human pluripotent stem cell culture under fully defined conditions. *Proc Natl Acad Sci U S A.* **108** (46), 18714-18719 (2011).
18. Bettinger, C. J., Langer, R., & Borenstein, J. T. Engineering substrate topography at the micro- and nanoscale to control cell function. *Angew Chem Int Ed Engl.* **48** (30), 5406-5415 (2009).
19. McMurray, R. J. *et al.* Nanoscale surfaces for the long-term maintenance of mesenchymal stem cell phenotype and multipotency. *Nat Mater.* **10** (8), 637-644 (2011).
20. Sun, Y., Jallerat, Q., Szymanski, J. M., & Feinberg, A. W. Conformal nanopatterning of extracellular matrix proteins onto topographically complex surfaces. *Nat Methods.* **12** (2), 134-136 (2015).
21. Nitanan, T. *et al.* Effects of processing parameters on morphology of electrospun polystyrene nanofibers. *Korean J Chem Eng.* **29** (2), 173-181, (2012).
22. Liu, L. *et al.* Chemically-defined scaffolds created with electrospun synthetic nanofibers to maintain mouse embryonic stem cell culture under feeder-free conditions. *Biotechnol Lett.* **34** (10), 1951-1957 (2012).
23. Liu, L. *et al.* Nanofibrous gelatin substrates for long-term expansion of human pluripotent stem cells. *Biomaterials.* **35** (24), 6259-6267 (2014).
24. Kamei, K. *et al.* Phenotypic and transcriptional modulation of human pluripotent stem cells induced by nano/microfabrication materials. *Adv Healthcare Mater.* **2** (2), 287-291 (2013).
25. Peerani, R. *et al.* Niche-mediated control of human embryonic stem cell self-renewal and differentiation. *EMBO J.* **26** (22), 4744-4755 (2007).
26. Yamamoto, K. *et al.* Fluid shear stress induces differentiation of Flk-1-positive embryonic stem cells into vascular endothelial cells in vitro. *Am J Physiol Heart Circ Physiol.* **288** (4), H1915-1924 (2005).
27. Charati, S. G., & Stern, S. A. Diffusion of gases in silicone polymers: Molecular dynamics simulations. *Macromolecules.* **31** (16), 5529-5535 (1998).
28. Prado-Lopez, S. *et al.* Hypoxia promotes efficient differentiation of human embryonic stem cells to functional endothelium. *Stem Cells.* **28** (3), 407-418 (2010).
29. Yanagihara, K. *et al.* Prediction of Differentiation Tendency Toward Hepatocytes from Gene Expression in Undifferentiated Human Pluripotent Stem Cells. *Stem Cells and Development.* **25** (24), 1884-1897 (2016).
30. Kamei, K. *et al.* 3D printing of soft lithography mold for rapid production of polydimethylsiloxane-based microfluidic devices for cell stimulation with concentration gradients. *Biomed Microdevices.* **17** (2) (2015).
31. Song, J. H., Kim, H. E., & Kim, H. W. Production of electrospun gelatin nanofiber by water-based co-solvent approach. *J Mater Sci Mater Med.* **19** (1), 95-102 (2008).
32. Owen, M. J., & Smith, P. J. Plasma Treatment of Polydimethylsiloxane. *J Adhes Sci Technol.* **8** (10), 1063-1075 (1994).
33. Chen, G. K. *et al.* Chemically defined conditions for human iPSC derivation and culture. *Nat Methods.* **8** (5), 424-476 (2011).
34. Watanabe, K. *et al.* A ROCK inhibitor permits survival of dissociated human embryonic stem cells. *Nat Biotechnol.* **25** (6), 681-686 (2007).
35. Kamei, K. *et al.* An integrated microfluidic culture device for quantitative analysis of human embryonic stem cells. *Lab Chip.* **9** (4), 555-563 (2009).
36. Kamei, K. *et al.* Microfluidic image cytometry for quantitative single-cell profiling of human pluripotent stem cells in chemically defined conditions. *Lab Chip.* **10** (9), 1113-1119 (2010).
37. Carpenter, A. E. *et al.* CellProfiler: image analysis software for identifying and quantifying cell phenotypes. *Genome Biol.* **7** (10), R100 (2006).
38. Kohonen, T. Self-Organized Formation of Topologically Correct Feature Maps. *Biol Cybern.* **43** (1), 59-69 (1982).
39. Wehrens, R., & Buydens, L. M. C. Self- and super-organizing maps in R: The kohonen package. *J Stat Softw.* **21** (5), 1-19 (2007).
40. Eisen, M. B., Spellman, P. T., Brown, P. O., & Botstein, D. Cluster analysis and display of genome-wide expression patterns. *Proc Natl Acad Sci U S A.* **95** (25), 14863-14868 (1998).
41. Saldanha, A. J. Java Treeview--extensible visualization of microarray data. *Bioinformatics.* **20** (17), 3246-3248 (2004).
42. Du, G. S., Fang, Q., & den Toonder, J. M. J. Microfluidics for cell-based high throughput screening platformsd-A review. *Anal Chim Acta.* **903** 36-50 (2016).
43. Huang, S. B. *et al.* An integrated microfluidic cell culture system for high-throughput perfusion three-dimensional cell culture-based assays: effect of cell culture model on the results of chemosensitivity assays dagger. *Lab Chip.* **13** (6), 1133-1143 (2013).
44. Wang, B. L. *et al.* Microfluidic high-throughput culturing of single cells for selection based on extracellular metabolite production or consumption. *Nat Biotechnol.* **32** (5), 473-U194 (2014).
45. Becker, K. A. *et al.* Self-renewal of human embryonic stem cells is supported by a shortened G1 cell cycle phase. *J Cell Physiol.* **209** (3), 883-893 (2006).
46. Neganova, I., & Lako, M. G1 to S phase cell cycle transition in somatic and embryonic stem cells. *J Anat.* **213** (1), 30-44 (2008).
47. Fox, V. *et al.* Cell-cell signaling through NOTCH regulates human embryonic stem cell proliferation. *Stem Cells.* **26** (3), 715-723 (2008).
48. Xu, C. *et al.* Feeder-free growth of undifferentiated human embryonic stem cells. *Nat Biotechnol.* **19** (10), 971-974 (2001).
49. Kamei, K. *et al.* Microfluidic-Nanofiber Hybrid Array for Screening of Cellular Microenvironments. *Small.* **13**, (18), 1603104, (2017).

50. Sun, J. *et al.* A Microfluidic Platform for Systems Pathology: Multiparameter Single-Cell Signaling Measurements of Clinical Brain Tumor Specimens. *Cancer Res.* **70** (15), 6128-6138 (2010).
51. Theunissen, T. W., & Jaenisch, R. Molecular Control of Induced Pluripotency. *Cell Stem Cell.* **14** (6), 720-734 (2014).
52. Yoo, H. S., Kim, T. G., & Park, T. G. Surface-functionalized electrospun nanofibers for tissue engineering and drug delivery. *Adv Drug Del Rev.* **61** (12), 1033-1042 (2009).
53. Dixon, J. E. *et al.* Combined hydrogels that switch human pluripotent stem cells from self-renewal to differentiation. *Proc Natl Acad Sci U S A.* **111** (15), 5580-5585 (2014).

